energies

MDPI

Article

Analysis and Experiment for Wireless Power Transfer Systems with Two Kinds Shielding Coils in EVs

Yushan Wang [1,2,*], Baowei Song [1] and Zhaoyong Mao [1,2]

[1] School of Marine Science and Technology, Northwestern Polytechnical University, Xi'an 710072, China; songbaowei@nwpu.edu.cn (B.S.); maozhaoyong@nwpu.edu.cn (Z.M.)

[2] Key Laboratory for Unmanned Underwater Vehicle, Northwestern Polytechnical University, Xi'an 710072, China

* Correspondence: yushanwang@mail.nwpu.edu.cn; Tel.: +86-153-1999-6991

Received: 28 November 2019; Accepted: 31 December 2019; Published: 6 January 2020

Abstract: Electric vehicles (EVs) with wireless power transfer (WPT) systems are convenient, but WPT technology will produce a strong stray electromagnetic field (EMF) in the surrounding space when the system works with high power. Shielding coils can reduce stray EMF efficiently without additional control, and they have advantages of being simple, light, and cheap. In this paper, the series-opposing structure is compared systematically with the inductive structure based on circuit theory and electromagnetic field theory. Simplified circuit models are proposed to give an intuitive and comprehensive analysis of transfer efficiency. Electric field analysis and finite element analysis (FEA) is used to explain the functional principles of shielding coils and to compare the EMF distribution excited by two structures. The simulation results show that both structures decrease the mutual inductance and perform better than the system without shielding coils when they have the same transfer efficiency. Further, the inductive structure system performs best. The most important between two structures is that the shielding effects is independent of turns of shielding coils for inductive structure, while it can be adjusted by changing turns of shielding coils for the series-opposing structure. The experimental results show that the EMF is reduced by 65% for the inductive structure and 40% for the series-opposing structure. The theoretical analysis is confirmed by experimental results.

Keywords: wireless power transfer (WPT); electric vehicles (EVs); electromagnetic field (EMF); finite element analysis (FEA)

1. Introduction

Due to air pollution and the reduction of fossil fuel consumption, electric vehicles (EVs) have attracted much attention over the past two decades. The energy supply method for EVs is cable plug-in type at present. This method requires sufficient friction and cannot realize dynamic charging. Wireless power transfer (WPT) technology shows great potential for the advantage of convenience, and it has been widely used in many areas, such as electric vehicles, consumer electronics, implantable medical devices, and autonomous underwater vehicles [1,2]. X. Dai et al. [3] presented a method that takes almost all requirements for maximum tracking into account, including adaption for coupling coefficient, load variation, and output controllability. The method can achieve a good performance against parameter variation in dynamic charging. Furthermore, researchers provided a dynamic EV charging system for traffic applications and the system was conducted at 5 kW within the lateral misalignment of ±200 mm in [4]. For a WPT system to be used in clinical environment, Ref. [5] gave priority consideration to three technical difficulties, i.e., implantation, efficiency, and safety with the LCC-C compensation topology. For the underwater environment, researchers designed a WPT system for underwater vehicles and realized charging power of 300 W with the efficiency from 75% to 91%

in [6]. In addition, A three-phase WPT system was designed and analyzed in [7]. The structure has good eccentricity resistance and is able to transfer 1.0 kW with the efficiency of 92.41%. With the continuous breakthrough of key technologies, WPT systems will be applied in an increasing number of fields.

WPT technology based on electromagnetic field theory represents one of the most attractive WPT approaches and such technology produces stray EMF in the surrounding space during work conditions. In the future, power transfer capability will realize tens of kilowatts, and it will bring strong stray EMF which is harmful to humans and demonstrates a severe influence on peripheral electric equipment. Researchers proposed several methods to reduce stray EMF, such as the magnetic shield, metal shield, shielding coils, and controlling windings phase. Metal shield is always applied together with the magnetic shield. The method attenuates the stray EMF effectively, but the metal plate can reduce the mutual inductance and power transmission efficiency when magnetic cores aren't used. The variation law of a coil's equivalent inductance and resistance is deduced when the coil is surrounded by the non-ferromagnetic metal plate in paper [8]. Besides, researchers optimized the EMF shielding method considering shielding effectiveness associated with system performance by metallic sheets in paper [9]. The weak points of the metal shield and magnetic shield are apparent and serious. The weight of couplers was increased significantly to make the WPT system inflexible and their expense is high. The method of controlling winding phase will not increase the couplers' size and weight. Researchers found that the stray EMF was reduced by up to 30% when the phase difference is 50° between the transmitter current and receiver current in paper [10]. However, this has an influence on the efficiency of the inverter, and the control strategy becomes more complex. Shielding coils effectively decrease stray EMF with simple implementation and have light influence on coupler structure and system transmission efficiency. Further, shielding coils attenuate stray EMF without additional control and they have advantages as, light and cheap. In paper [11], four kinds of shielding method including plate shield, ring shield, litz shield and reverse loops were compared using Pareto fronts of efficiency verse stray EMF. And they found that the stray EMF was attenuated by 75% in the experiment using litz shield. The pity is that there are only some compared results, without systematic analysis and functional principles. The series-opposing structure and the inductive structure are the most used style of shielding coils. In order to learn the difference between these two attractive structures and know well about their characteristics, the rule of shielding effectiveness, we made the comparative study between them based on circuit theory and electromagnetic field theory.

The series-opposing structure means that the shielding coils are series connection with power transmission coils in reversed clockwise direction. So, the current in power transmission coils and shielding coils is in a totally reversed direction and have the same modulus value. The EMF generated by power transmission coils and shielding coils is in opposed direction in the stray region. Figure 1a shows the working principle of the series-opposing structure. The principle of the inductive structure is similar to the series-opposing structure, but the current in shielding coils is inductive from power transmission coils as illustrated in Figure 1b and its position has an influence on the current value. Briefly, these two structures make use of EMF excited by shielding to reduce the stray field.

When the coils and the transmission distance are same, the difference between these two structures is that the current in shielding coils possess a different phase and amplitude. In this paper, we compared these two structures based on circuit theory. The analysis results show that shielding coils decrease the coupling coefficient and the transfer efficiency. When the ratio of the inductance between the main coils and the shielding coils satisfies certain conditions, the transfer efficiency is the same. The turns of shielding coils play an important role in the efficiency of the series-opposing structure and have little influence on the inductive structure. Further, the coupling coefficients about shielding coils affect the compensation capacitors selection. In addition, we analyzed the distribution of EMF in the surrounding space through finite element analysis (FEA) solution. The results show that both structures can reduce stray EMF and the inductive structure performs better than the series-opposing structure. The turns of shielding coils have an influence on the series-opposing structure and the

shielding effectiveness is constant for the inductive structure. We have carried out experiments and the experimental results show that the EMF is reduced by 65% for the inductive structure and 40% for the series-opposing structure when the turns of shielding coils are three. The theoretical analysis is confirmed by experimental results. On the basis of these research, we can grasp the characteristics and the rule of shielding effectiveness of these two kinds of shielding coils. It can help to choose the suitable shielding method in the engineering application.

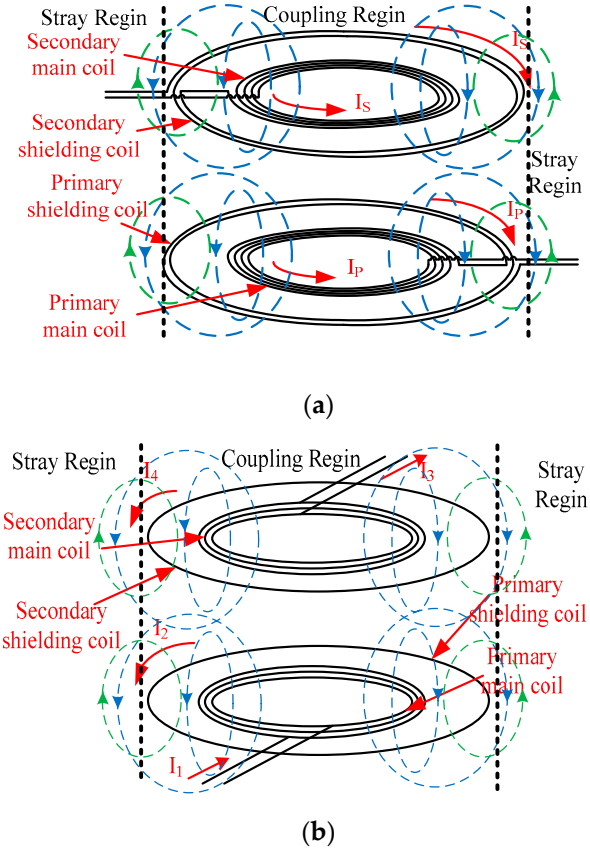

Figure 1. Working schematic diagram of shielding coils where the blue lines mean the EMF excited by power transmission coils and green lines mean the cancel EMF produced by shielding coils: (**a**) the series-opposing structure; (**b**) the inductive structure.

This paper is organized as follows: the circuit analysis of the series-opposing structure and the inductive structure are presented in Section 2. The FEA analysis and comparison of the EMF in the surrounding space for these two structure in Section 3. The experiments and are drawn in Section 4. Finally, Section 5 contains some concluding remarks.

2. Circuit Analysis

Researchers have proven that both coupled-mode theory and circuit theory have the same analysis results in a steady state for midrange transfer distance [12,13]. In this paper, the model based on circuit theory is used. The equivalent circuit models of common series-opposing and inductive structures for WPT systems are illustrated in Figure 2, where 1, 2, 3, and 4 denote the primary power transmission coil, primary shielding coil, secondary power transmission coil, and secondary shielding coil, respectively. Subscripts P and S mean the primary and secondary circuit, L is the inductance, C is the compensation capacitances which series connected with power transmission coils, U is the voltage source, R is the equivalent series resistance (ESR) of coils and the connection lines, R_L means the equivalent load

resistance, I denotes the current, M is the mutual inductance, P_{in} is the input power, and P_{out} is the output power. The difference between these two structures is the current in shielding coils.

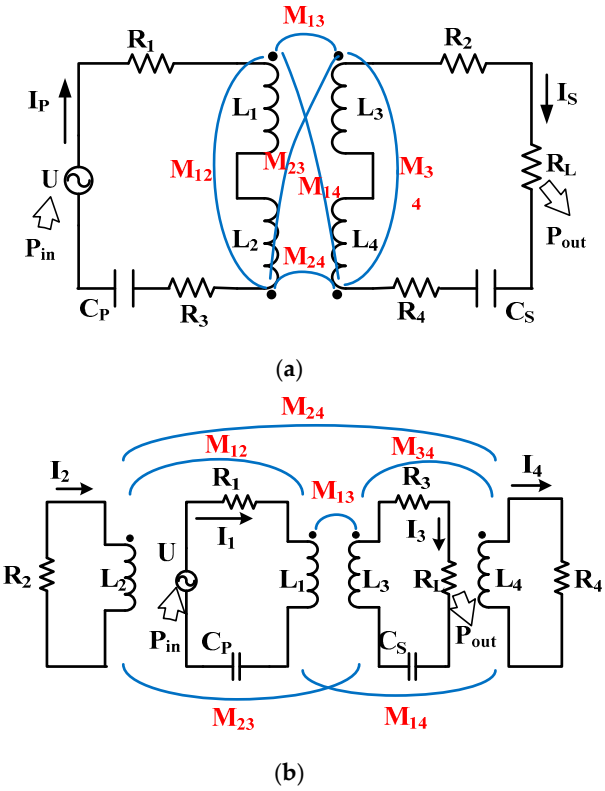

Figure 2. Equivalent circuit models for two kinds WPT systems with shielding coils: (**a**) the circuit model of series-opposing structure WPT systems; (**b**) the circuit model of inductive structure WPT systems.

For series-opposing structure WPT systems, Equations (1) and (2) can be obtained:

$$L_P = L_1 + L_2 - 2M_{12} \tag{1}$$

$$L_S = L_3 + L_4 - 2M_{34} \tag{2}$$

Assuming that $\vec{B}_1$ is the magnetic flux density and $\vec{S}$ is the equivalent area of the coil, we can get the magnetic flux from its definition:

$$\Phi_{PS} = \oint_{S_3} \vec{B}_1 d\vec{S} + \oint_{S_3} \vec{B}_2 d\vec{S} + \oint_{S_4} \vec{B}_1 d\vec{S} + \oint_{S_4} \vec{B}_2 d\vec{S} \tag{3}$$

From the definition of mutual inductance, we can get the expressions of these mutual inductance as:

$$M_{13} = \frac{\Phi_{13}}{I_P} = \frac{\oint_{S_3} \vec{B}_1 d\vec{S}}{I_P}, M_{23} = \frac{\oint_{S_3} \vec{B}_2 d\vec{S}}{-I_P}, M_{14} = \frac{\oint_{S_4} \vec{B}_1 d(-\vec{S})}{I_P}, M_{24} = \frac{\oint_{S_4} B_2 d(-\vec{S})}{-I_P} \tag{4}$$

Combining (3) and (4), it's easy to get the equivalent mutual inductance between the primary coils and the secondary coils.

$$M_{PS} = \frac{\Phi_{PS}}{I_P} = M_{13} - M_{14} - M_{23} + M_{24} \tag{5}$$

Based on Kirchhoff's law, the constraint equations of the series-opposing structure WPT systems can be obtained:

$$\begin{cases} U = (j\omega L_P + \frac{1}{j\omega C_P} + R_1 + R_2)I_P + j\omega M_{PS} I_S \\ 0 = (j\omega L_S + \frac{1}{j\omega C_S} + R_3 + R_4 + R_L)I_S + j\omega M_{PS} I_P \end{cases} \tag{6}$$

For the reason that R_2, R_4 is very small compared with R_1, R_3 and R_L, we assume that:

$$R_2 = R_4 = 0 \tag{7}$$

C_P and C_S are selected to resonate with L_P and L_S at the angular frequency w respectively.

$$\omega = \frac{1}{\sqrt{L_P C_P}} = \frac{1}{\sqrt{L_S C_S}} \tag{8}$$

Combining Equations (6)–(8), we can get the expression of I_S and the equivalent resistance of the secondary circuit R_{ref}:

$$I_S = \frac{j\omega M_{PS} I_P}{R_3 + R_L} \tag{9}$$

$$R_{ref} = |\frac{j\omega M_{PS} I_S}{I_P}| = \frac{\omega^2 M_{PS}^2}{R_3 + R_L} \tag{10}$$

Using (10), the current of the primary circuit can be calculated by:

$$I_P = \frac{U}{R_1 + R_{ref}} = \frac{U(R_3 + R_L)}{R_1(R_3 + R_L) + \omega^2 M_{PS}^2} \tag{11}$$

The current of secondary circuit, input power, transfer efficiency and output power can be obtained as:

$$I_S = \frac{j\omega M_{PS} U}{R_1(R_3 + R_L) + \omega^2 M_{PS}^2} \tag{12}$$

$$P_{in} = UI_P = \frac{U^2}{R_1 + R_{ref}} = \frac{U^2(R_3 + R_L)}{R_1(R_3 + R_L) + \omega^2 M_{PS}^2} \tag{13}$$

$$P_{out} = I_S^2 R_L = \frac{R_L U^2 \omega^2 M_{PS}^2}{\left(R_1(R_3 + R_L) + \omega^2 M_{PS}^2\right)^2} \tag{14}$$

$$\eta = \frac{R_{ref}}{R_{ref} + R_1}\frac{R_L}{R_L + R_3} = \frac{R_L}{R_3 + R_L}\frac{\omega^2 M_{PS}^2}{R_1(R_3 + R_L) + \omega^2 M_{PS}^2} \tag{15}$$

Before analyzing the inductive structure WPT system, we simplify the expressions of the impedance Z of the four circuits as:

$$\begin{cases} Z_1 = R_1 + j\omega L_1 + 1/j\omega C_P \\ Z_2 = R_2 + j\omega L_2 \\ Z_3 = R_3 + j\omega L_3 + 1/j\omega C_S + R_L \\ Z_4 = R_4 + j\omega L_4 \end{cases} \tag{16}$$

Similar to the opposing-series structure WPT system, we can get the equivalent equations:

$$\begin{cases} U = Z_1 I_1 + j\omega(M_{12} I_2 + M_{13} I_3 + M_{14} I_4) \\ 0 = Z_2 I_2 + j\omega(M_{12} I_1 + M_{23} I_3 + M_{24} I_4) \\ 0 = Z_3 I_3 + j\omega(M_{13} I_1 + M_{23} I_2 + M_{34} I_4) \\ 0 = Z_4 I_4 + j\omega(M_{14} I_1 + M_{24} I_2 + M_{34} I_3) \end{cases} \tag{17}$$

Because the working frequency is high, the modulus of the imaginary part is much larger than that of the real part of Z_2 and Z_4. The R_2 and R_4 are negligible, and we can get:

$$\begin{cases} Z_2 = j\omega L_2 \\ Z_4 = j\omega L_4 \end{cases} \tag{18}$$

From the definition of the coupling coefficient, the coupling coefficient can be calculated as:

$$k_{xy} = M_{xy} / \sqrt{L_x L_y} \tag{19}$$

Substituting Equations (18) and (19) in (17), the expression of I_3 can be obtained as:

$$I_3 = -\frac{k_{13}k_{24}^2 - k_{14}k_{23}k_{24} - k_{12}k_{24}k_{34} + k_{12}k_{23} + k_{14}k_{34} - k_{13}}{(k_{23}^2 - 2k_{23}k_{24}k_{34} + k_{34}^2)L_3 + Z_3(j\omega)^{-1}(k_{24}^2 - 1)} \sqrt{L_1 L_3} I_1 \tag{20}$$

From the expression of the I_3, we select the C_S to make sure the secondary circuit in resonance state:

$$C_S = \frac{1 - k_{24}^2}{(1 + 2k_{23}k_{24}k_{34} - k_{23}^2 - k_{34}^2 + k_{24}^2)\omega^2 L_3} \tag{21}$$

When the secondary circuit in resonance state, we can get the expressions of I_3, I_2 and I_4.

$$I_3 = -\frac{j\omega\sqrt{L_1 L_3}}{(1 - k_{24}^2)(R_3 + R_L)}(k_{13}(1 - k_{24}^2) + k_{14}k_{23}k_{24} + k_{12}k_{24}k_{34} - k_{12}k_{23} - k_{14}k_{34})I_1 \tag{22}$$

$$I_2 = \frac{k_{14}k_{24} - k_{12}}{1 - k_{24}^2}\sqrt{\frac{L_1}{L_2}}I_1 + \frac{k_{24}k_{34} - k_{23}}{1 - k_{24}^2}\sqrt{\frac{L_3}{L_2}}I_3 \tag{23}$$

$$I_4 = \frac{k_{12}k_{24} - k_{14}}{1 - k_{24}^2}\sqrt{\frac{L_1}{L_4}}I_1 + \frac{k_2k_{24} - k_{34}}{1 - k_{24}^2}\sqrt{\frac{L_3}{L_4}}I_3 \tag{24}$$

The equivalent impedances of circuits 2, 3, and 4 can be obtained as:

$$Z_{13} = \frac{j\omega M_{13}I_3}{I_1} = j\omega k_{13}\sqrt{L_1 L_3}\frac{I_3}{I_1} \tag{25}$$

$$Z_{12} = \frac{j\omega_0 M_{12}I_2}{I_1} = \frac{j\omega L_1 k_{12}(k_{14}k_{24} - k_{12})}{1 - k_{24}^2} + \frac{j\omega k_{12}(k_{24}k_{34} - k_{23})\sqrt{L_1 L_3}}{1 - k_{24}^2}\frac{I_3}{I_1} \tag{26}$$

$$Z_{14} = \frac{j\omega_0 M_{14}I_4}{I_1} = \frac{j\omega L_1 k_{14}(k_{12}k_{24} - k_{14})}{1 - k_{24}^2} + \frac{j\omega k_{14}(k_{23}k_{24} - k_{34})\sqrt{L_1 L_3}}{1 - k_{24}^2}\frac{I_3}{I_1} \tag{27}$$

The expression of I_1 is:

$$I_1 = \frac{U}{Z_1 + Z_{12} + Z_{13} + Z_{14}} \tag{28}$$

Substituting Equations (16), (25)–(27) in (28), we can get the denominator of I_1.

$$De(I_1) = R_1 + \frac{1}{j\omega C_P} + \frac{j\omega L_1(1 - k_{24}^2 + k_{12}k_{14}k_{24} - k_{12}^2 - k_{14}^2)}{1 - k_{24}^2} + j\omega\sqrt{L_1 L_3}\frac{I_3}{I_1}\left(\frac{k_{12}(k_{24}k_{34} - k_{23})}{1 - k_{24}^2} + k_{13} + \frac{k_{14}(k_{23}k_{24} - k_{34})}{1 - k_{24}^2}\right) \tag{29}$$

Bring Equation (22) into (29), it can be obtained that:

$$De(I_1) = R_1 + \frac{1}{j\omega C_P} + \frac{j\omega L_1(1 - k_{24}^2 + k_{12}k_{14}k_{24} - k_{12}^2 - k_{14}^2)}{1 - k_{24}^2} + \frac{\omega^2}{R_3 + R_L}\left[\left(\frac{k_{12}(k_{24}k_{34} - k_{23})}{1 - k_{24}^2} + k_{13} + \frac{k_{14}(k_{23}k_{24} - k_{34})}{1 - k_{24}^2}\right)\sqrt{L_1 L_3}\right]^2 \tag{30}$$

From Equation (30), we can get the resonance condition for circuit 1.

$$C_P = \frac{1-k_{24}^2}{(1-k_{12}^2-k_{14}^2-k_{24}^2+2k_{12}k_{14}k_{24})\omega^2 L_1} \tag{31}$$

In order to make the analysis easy, we define k_{eq} as (32) and get the expression of M_{eq}:

$$k_{eq} = \frac{k_{12}(k_{24}k_{34}-k_{23})}{1-k_{24}^2} + k_{13} + \frac{k_{14}(k_{23}k_{24}-k_{34})}{1-k_{24}^2} \tag{32}$$

$$M_{eq} = k_{eq}\sqrt{L_1 L_3} = M_{13} + \frac{k_{12}(k_{24}k_{34}-k_{23})+k_{14}(k_{23}k_{24}-k_{34})}{1-k_{24}^2}\sqrt{L_1 L_3} \tag{33}$$

When the C_P is selected to make sure the circuit 1 be in resonance condition, we can get expressions of the current in circuit 1 and circuit 3 from Equations (22) and (28).

$$I_1 = \frac{U(R_3+R_L)}{R_1(R_3+R_L)+\omega^2 M_{eq}^2} \tag{34}$$

$$I_3 = -\frac{j\omega M_{eq} U}{(R_3+R_L)R_1+\omega^2 M_{eq}^2} \tag{35}$$

The input power P_{in}, output power P_{out} and the transfer efficiency η can be calculated:

$$P_{in} = UI_1 = \frac{U^2(R_3+R_L)}{R_1(R_3+R_L)+\omega^2 M_{eq}^2} \tag{36}$$

$$P_{out} = R_L I_3^2 = \frac{R_L U^2 \omega^2 M_{eq}^2}{\left(R_1(R_3+R_L)+\omega^2 M_{eq}^2\right)^2} \tag{37}$$

$$\eta = \frac{P_{out}}{P_{in}} = \frac{R_L}{R_3+R_L}\frac{\omega^2 M_{eq}^2}{R_1(R_3+R_L)+\omega^2 M_{eq}^2} \tag{38}$$

From Equations (5) and (33), it is easy to find that the existence of shielding coils lowering the equivalent inductance. Comparing Equations (11)–(15) with (34)–(38), it is obvious that the difference between the series-opposing structure and the inductive structure is the expression of the equivalent mutual inductance. Further, expressions of C_P and C_S are different. From Equations (5) and (33), it can be observed that M_{PS} changes with coupling coefficients, inductance of power transmission coils and shielding coils. However, the inductance of shielding coils has no influence on M_{eq}. This means that we can't adjust M_{eq} through changing the turn of shielding coils when the coupling coefficients keep constant.

In general, coils are symmetrically distributed. We can obtain:

$$L_1 = L_3, L_2 = L_4, M_{12} = M_{34}, M_{14} = M_{23} \tag{39}$$

Make M_{PS} be equal to M_{eq}, it can be obtained that:

$$M_{PS} = M_{eq} \tag{40}$$

$$\frac{L_2}{L_1} - 2\frac{k_{14}}{k_{24}}\sqrt{\frac{L_2}{L_1}} + \frac{2k_{12}k_{14}-k_{24}(k_{12}^2+k_{14}^2)}{k_{24}(1-k_{24}^2)} = 0 \tag{41}$$

There are two solutions of Equation (41). Considering the inductance of transmission coils is larger than shielding coils, we choose the smaller as the real result. Then, we can get the break point O.

$$O = \sqrt{\frac{L_2}{L_1}} = \frac{k_{14}}{k_{24}} - \sqrt{\frac{k_{14}^2}{k_{24}^2} - \frac{2k_{12}k_{14} - k_{24}(k_{12}^2 + k_{14}^2)}{k_{24}(1 - k_{24}^2)}} \tag{42}$$

Because transmission coils are the main coils, we make sure $L_1 > 2L_2$. In order to facilitate comparative studies, we set up the following. The transmission coils are 15 turns, and their inner and outer diameters are 311 mm and 515 mm; the shielding coils' inner and outer diameters are 605 mm and 669 mm; the transmission distance is 100 mm; the radius of the coils line is 2 mm. According to these parameters and making use of the software Comsol5.4, we can get that: $L_1 = L_3 = 125.95$ μH; $L_2 = L_4 = 1.43\ n^2$μH where n is the turns of shielding coils; $k_{12} = k_{34} = 0.356$; $k_{13} = 0.358$; $k_{14} = k_{23} = 0.250$; $k_{24} = 0.323$.

Based on the coils' inductance and these coupling coefficients, we can get the relationship between the turn of shielding coils and the equivalent mutual inductance for the series-opposing structure system and the inductive structure system from Equations (5) and (33). The results are illustrated in Figure 3.

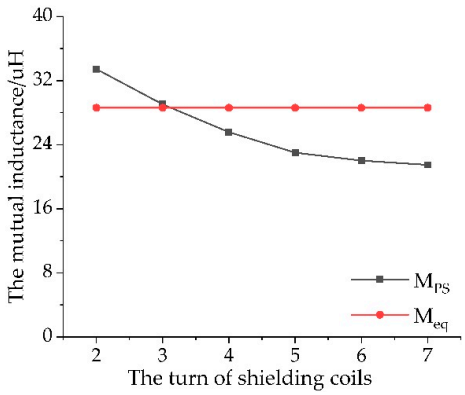

Figure 3. M_{PS} and M_{eq} change with the turn of shielding coils.

Based on the simulation results about M_{PS}, M_{eq}, R_1, R_2, R_3, R_4 and these coupling coefficients, we get the transmission characteristics of WPT systems. The relationships between efficiency, output power, and the equivalent mutual inductance, in terms of frequency is presented in Figure 4.

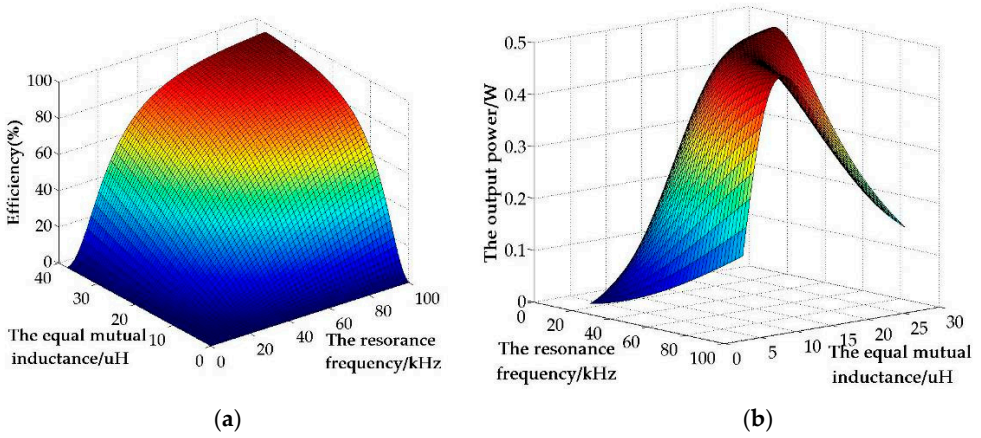

(**a**) (**b**)

Figure 4. Transmission characteristics for WPT system: (**a**) the power transmission efficiency changes with the resonance frequency and equivalent mutual inductance; (**b**) the output power changes with the resonance frequency and equivalent mutual inductance when $U = 1$ V.

From Figure 3, it is very clear that M_{eq} doesn't change with the turn of shielding coils and M_{PS} decreases first and then increase with the increases of the turn of shielding coils. But with its turn increasing, shielding coils can't play the role of shields. So, in general, M_{PS} decreases with the increasing of shielding coils' turn. The simulation results confirmed the results of circuit analysis.

Figure 4 shows the transmission characteristics of WPT systems. The equivalent mutual inductance has great effects on transmission efficiency and output power. So, the results shown in Figure 3 mean that the turn of shielding coils can't affect the transmission characteristics of the inductive structure, but it is one of the key roles for the series-opposing structure system. Shielding coils will reduce the equivalent mutual inductance, so it can be treated as the cost of reducing stray EMF.

3. Electric Field Analysis

In Figure 5, human or the electronics may be exposed in Area I, so we choose the stray EMF in Area I as the analysis target. From paper [14,15], we can get that the electric field excited by a single-turn circular coil can be calculated with Equation (43) and the method is proven by researchers.

$$\vec{E}(\rho,\varphi,z) = \vec{E}_{\phi}(\rho,\varphi,z) = -j\omega\mu aI\int_0^{\infty}\frac{\lambda}{u}J_1(\lambda a)J_1(\lambda\rho)e^{-u|z|}d\lambda\cdot\vec{e}_{\phi} \tag{43}$$

$$u = \sqrt{\lambda^2-\omega\mu(\omega\varepsilon-j\sigma)} \tag{44}$$

$$\vec{H} = -\frac{1}{j\omega\mu}\nabla\times(\vec{E}) \tag{45}$$

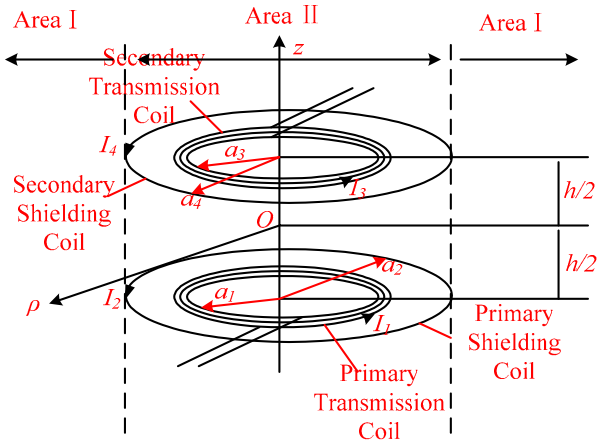

Figure 5. The structure for WPT system with shielding coils.

In Equation (43), a is the radius of the coil, I is the current in coil and μ, ε, σ are the permeability, permittivity and conductivity of the transmission medium respectively. J_1 is the first kind and first order Bessel function.

From (45), we can find that the modulus of $\vec{E}$ and $\vec{H}$ is a linear relation and they change in the same way. It is unnecessary that studying electric field and magnetic field respectively. We can treat the changing rule of electric field as the changing rule of EMF. The electric field excited by the WPT system coils is the vector sum of the electric field excited by every coils. So, we can calculate $\vec{E}$ with the Equation (46).

$$\vec{E} = \sum_{i=1}^{m}\vec{E}_i\, i = 1,2,3,4 \tag{46}$$

From the previous part, the currents in circuit 2 and circuit 4 for the inductive structure can be calculated:

$$I_2 = \left(\frac{k_{14}k_{24} - k_{12}}{1 - k_{24}^2} + \frac{j\omega M_{13}}{R_3 + R_L} \frac{k_{12}k_{24} - k_{14}}{1 - k_{24}^2} \right) \sqrt{\frac{L_1}{L_2}} I_1 \tag{47}$$

$$I_4 = \left(\frac{k_{12}k_{24} - k_{14}}{1 - k_{24}^2} + \frac{j\omega M_{13}}{R_3 + R_L} \frac{k_{14}k_{24} - k_{12}}{1 - k_{24}^2} \right) \sqrt{\frac{L_1}{L_2}} I_1 \tag{48}$$

For the series-opposing structure WPT systems, we can get:

$$\begin{aligned} \dot{E} = & -j\omega\mu I_P \sum_{i=1}^{i=N_1} a_{1i} \int_0^\infty \tfrac{\lambda}{u} J_1(\lambda a_{1i}) J_1(\lambda\rho) e^{-u|z+\frac{h}{2}|} d\lambda \cdot \dot{e}_\phi + j\omega\mu I_P \sum_{i=1}^{i=N_2} a_{2i} \int_0^\infty \tfrac{\lambda}{u} J_1(\lambda a_{2i}) J_1(\lambda\rho) e^{-u|z+\frac{h}{2}|} d\lambda \cdot \dot{e}_\phi \\ & -j\omega\mu I_S \sum_{i=1}^{i=N_3} a_{3i} \int_0^\infty \tfrac{\lambda}{u} J_1(\lambda a_{3i}) J_1(\lambda\rho) e^{-u|z-\frac{h}{2}|} d\lambda \cdot \vec{e}_\phi + j\omega\mu I_S \sum_{i=1}^{i=N_3} a_{4i} \int_0^\infty \tfrac{\lambda}{u} J_1(\lambda a_{4i}) J_1(\lambda\rho) e^{-u|z-\frac{h}{2}|} d\lambda \cdot \vec{e}_\phi \end{aligned} \tag{49}$$

For the inductive structure WPT systems, we can get:

$$\begin{aligned} \vec{E} = & -j\omega\mu I_1 \sum_{i=1}^{i=N_1} a_{1i} \int_0^\infty \tfrac{\lambda}{u} J_1(\lambda a_{1i}) J_1(\lambda\rho) e^{-u|z+\frac{h}{2}|} d\lambda \cdot \vec{e}_\phi - j\omega\mu I_2 \sum_{i=1}^{i=N_2} a_{2i} \int_0^\infty \tfrac{\lambda}{u} J_1(\lambda a_{2i}) J_1(\lambda\rho) e^{-u|z+\frac{h}{2}|} d\lambda \cdot \vec{e}_\phi \\ & -j\omega\mu I_3 \sum_{i=1}^{i=N_3} a_{3i} \int_0^\infty \tfrac{\lambda}{u} J_1(\lambda a_{3i}) J_1(\lambda\rho) e^{-u|z-\frac{h}{2}|} d\lambda \cdot \vec{e}_\phi - j\omega\mu I_4 \sum_{i=1}^{i=N_4} a_{4i} \int_0^\infty \tfrac{\lambda}{u} J_1(\lambda a_{4i}) J_1(\lambda\rho) e^{-u|z-\frac{h}{2}|} d\lambda \cdot \vec{e}_\phi \end{aligned} \tag{50}$$

From the expressions of $\vec{E}$, it's easy to learn that: $\vec{E}$ is a linear correlation with the product of the turn and current when the coupling coefficients keep constant. For the series-opposing structure WPT system, the I_P in primary circuit increases with the inductance of shielding coils increasing, so the EMF excited by shielding coils will become stronger and stronger when the turn of shielding coils is within normal range. From the reason that $L \infty n^2$, combining (47), (48) and (50), we can learn that the product of shielding coils' turn and current keeps constant in the inductive structure. The EMF produced by shielding coil won't change with turn changing in inductive structure generally.

In order to observe the strength of the electric field around WPT system with or without shielding coils, we make use of MATLAB. The transmission distance is 100 mm and the radius of the coils line is 2 mm. The parameters about coils are obtained from simulation software Comsol5.4. We assume that $R_L = 50\ \Omega$; $R_1 = R_3 = 0.5\ \Omega$, $n = 5$. From Equations (43)–(45), we can obtain that the frequency have the same effect on different systems if their transmission medium is same, so we make f = 150 kHz. By making use of MATLAB and Equations (43)–(45), and making sure the system is in resonance state and $I_P = I_3 = 1$ A, we can get the distribution of the electric field as shown in Figure 6.

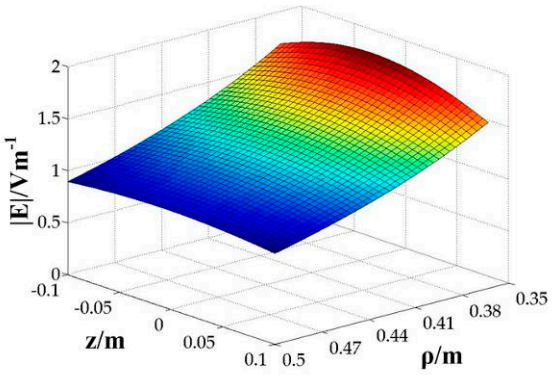

(**a**)

Figure 6. *Cont.*

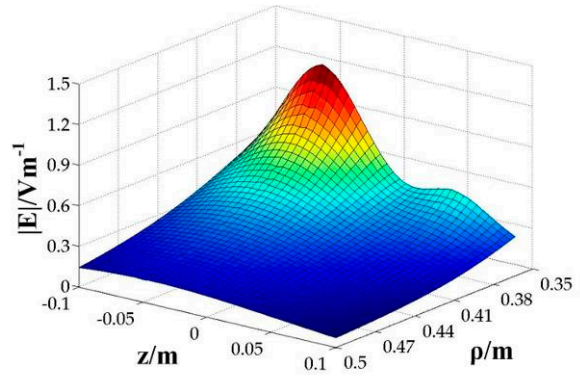

(**b**)

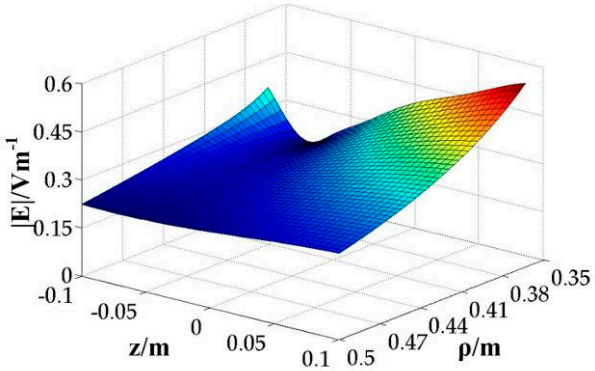

(**c**)

Figure 6. The electric field strength around WPT systems: (**a**) the WPT system without shielding coils; (**b**) the series-opposing structure WPT system; (**c**) the inductive structure WPT system.

From Figure 6, it is obtained that the shielding coils can reduce the EMF excited by the WPT system effectively. Further, when $n = 5$, the highest EMF point around inductive structure WPT system is about half of the EMF point around the series-opposing structure WPT system for the strongest point in Area *I*.

In order to analyze the relationship between the turns of shielding coils and the EMF, we make use of the software Comsol5.4. The parameters setting is the same as the previous part. Considering the frequency will not change the distribution of electric field and the power transmission can't be very small or very close, we make sure $f = 150$ kHz. Changing the turn of the power transmission coils or shielding coils, keeping the ESR of the connection line is 0.3 Ω, the output current being 1 A and the system in resonance state, we can get the electric field distribution. For the WPT system without shielding coils, we get the electric field distribution by changing turn of coils (keeping the distribution range or keeping the distance between adjacent turns constant) as a matched group.

Comparing Figure 7a–d, it is found that the EMF excited by the primary transmission coil becomes stronger and the EMF excited by the secondary transmission coil becomes weaker with power transmission coils' turn decreasing. The reason is that the current in the secondary circuit keep constant and the turn decreases. For the primary coil, the product of current and turn becomes large for the reason that the mutual inductance becomes less. In total, increasing the distance between adjacent turns or decreasing the turns has slight effects on the EMF distribution, but it will reduce the power transmission efficiency because the mutual inductance is decreased.

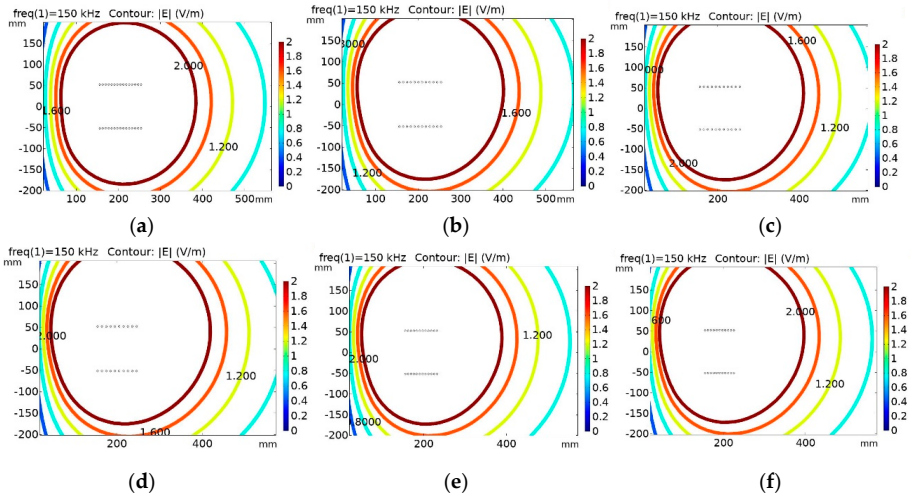

Figure 7. When the inner diameter is 311 mm, the power transmission efficiency η and EMF distribution which are from the WPT system without shielding coils changes with the turn of power transmission coils (N_p) and the distance between adjacent turns (d). (**a**) N_p = 15, d = 7 mm, η = 97.07% and the mutual inductance M = 45.06 μH. (**b**) N_p = 12, d = 8.91 mm, η = 95.74% and M = 28.86 μH. (**c**) N_p = 11, d = 9.8 mm, η = 94.76% and M = 24.24 μH; (**d**) N_p = 10, d = 10.09 mm, η = 93.24% and M = 20.04 μH; (**e**) N_p = 12, d = 7 mm, η = 94.94% and M = 26.71 μH; (**f**) N_p = 11, d = 7 mm, η = 93.47% and M = 21.83 μH.

Comparing Figures 7 and 8, it can be found that the series-opposing structure WPT system produces weaker EMF comparing with the system without shielding coils. The EMF becomes weak first and then increases with the shielding coils' turn increasing. This phenomenon can be explained by the fact that EMF excited by shielding coils became stronger with the increasing of turn, so the EMF in space became weaker first. After the point at which the strength of EMF is zero, the EMF in inverse strengthens with the increasing of turn. Further, the equivalent mutual inductance decreases with the turn increasing, so the transmission efficiency decreases with the turn of shield coils increasing. The simulation results are consistent with the circuit analysis.

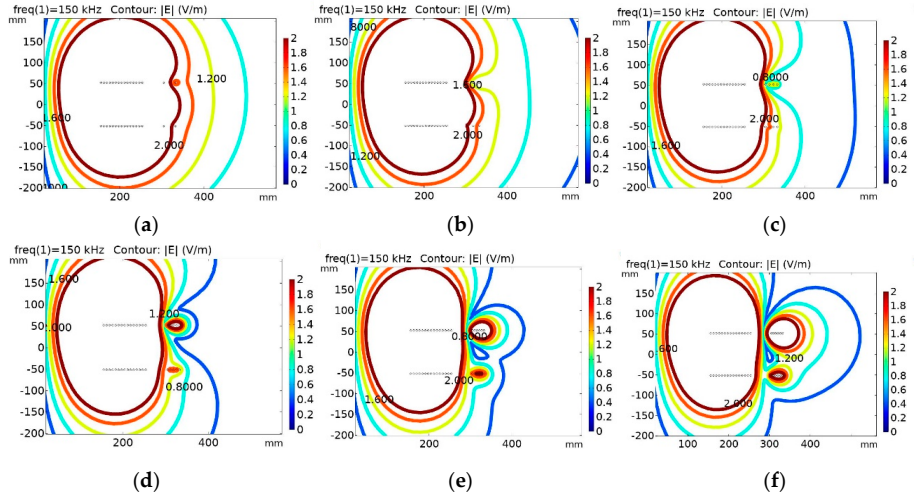

Figure 8. The power transmission efficiency η and EMF distribution which are from the WPT system with series-opposing shielding coils change with the turn of shielding coils(N_s): (**a**) N_p = 15, N_s = 2, η = 95.43% and M_{PS} = 33.21 μH; (**b**) N_p = 15, N_s = 3, η = 94.26% and M_{PS} = 28.99 μH; (**c**) N_p = 15, N_s = 4, η = 92.78% and M_{PS} = 25.56 μH; (**d**) N_s = 15, N_s = 5, η = 91.04% and M_{PS} = 23.01 μH; (**e**) N_p = 15, N_s = 6, η = 89.61% and M_{PS} = 22.01 μH; (**f**) N_p = 15, N_s = 7, η = 87.09% and M_{PS} = 20.68 μH.

From Figure 9, we can find that the EMF around the inductive structure WPT system and the transmission efficiency almost keep constant with the turn of shielding coils increasing. The reason for this phenomenon is that the product of the current and turn keeps constant for the shielding coils which we explained in the previous part. At the same time, the equal mutual inductance and the current in power transmission coils doesn't change with the turn of shielding coils. So, the EMF excited by the inductive structure WPT system doesn't change with the turn of shielding coils varying (n isn't equal to zero). The simulation results agree well with the circuit analysis.

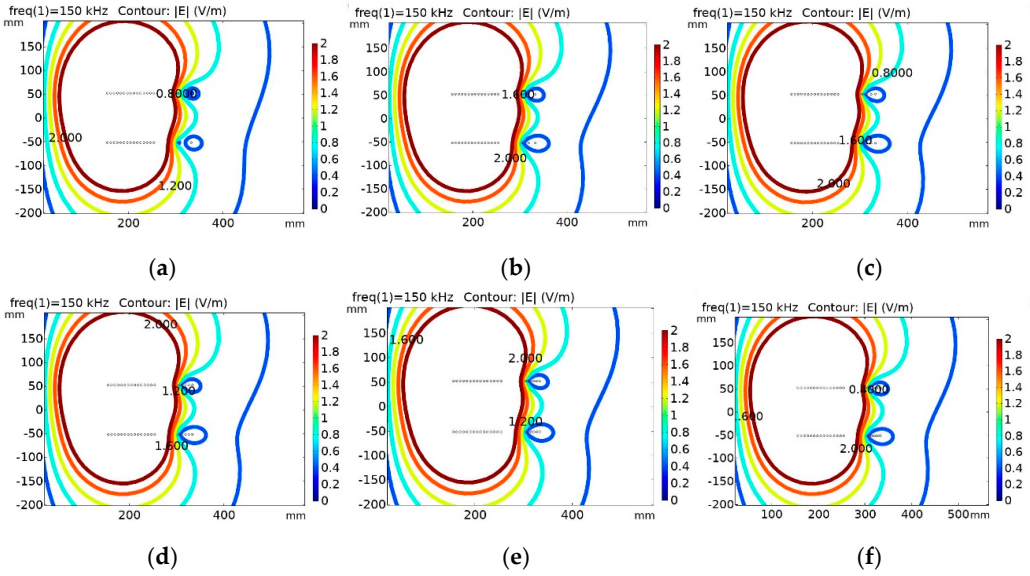

Figure 9. The power transmission efficiency η and EMF distribution which are from the WPT system with inductive shielding coils change with the turn of shielding coils (N_s): (**a**) $N_p = 15$, $N_s = 2$, $\eta = 94.18\%$ and $M_{eq} = 28.62$ μH; (**b**) $N_p = 15$, $N_s = 3$, $\eta = 94.27\%$ and $M_{eq} = 28.58$ μH; (**c**) $N_p = 15$, $N_s = 4$, $\eta = 94.30\%$ and $M_{eq} = 28.61$ μH; (**d**) $N_p = 15$, $N_s = 5$, $\eta = 94.28\%$ and $M_{eq} = 28.60$ μH; (**e**) $N_p = 15$, $N_s = 6$, $\eta = 94.19\%$ and $M_{eq} = 28.60$ μH; (**f**) $N_p = 15$, $N_s = 7$, $\eta = 93.95\%$ and $M_{eq} = 28.57$ μH.

Comparing Figure 7c, Figure 8b, and Figure 9, we can get the conclusion that when the power transmission efficiency are very close, the EMF excited by the structure with shielding coils is weaker than the structure without shielding coils, and the inductive structure WPT system performs best in these three systems.

In summary, shielding coils can reduce EMF effectively and they have slight influence on couplers' structure, so we should choose the structure with shielding coils first if the power transmission efficiency meets requirement considering body health and devices safe. The turns of shield coils affect performance of the series-opposing structure, so we can adjust the turn to make the EMF excited by WPT systems is weak enough. For the inductive WPT system, the transmission characteristics and the EMF won't change with the turn of shield coils, but the structure produces the least EMF when the transmission efficiency is same in these three structures. This means that if the EMF is weak enough, we'd better select the inductive structure WPT system.

4. Experiments and Discussion

In order to verify the aforementioned analysis results, we set up the experiment prototype illustrated in Figure 10. The power transmission coils, shielding coils and the measure coils are wound on the polymethyl methacrylate (PMMA) plate. By making use of the LCR analyzer, we can get the inductance and RES of coils and the mutual inductance between coils. The mutual inductance can be calculated in this way. Firstly, we get the total inductance L_{T1} of two coils (coil X and coil Y) series connection in the same direction and get the total inductance L_{T2} of the same coils series connection

in the reversed direction. From the inductance series connection rules, Equations (51) and (52) can be obtained.

$$L_{T1} = L_X + L_Y + 2M_{XY} \tag{51}$$

$$L_{T1} = L_X + L_Y - 2M_{XY} \tag{52}$$

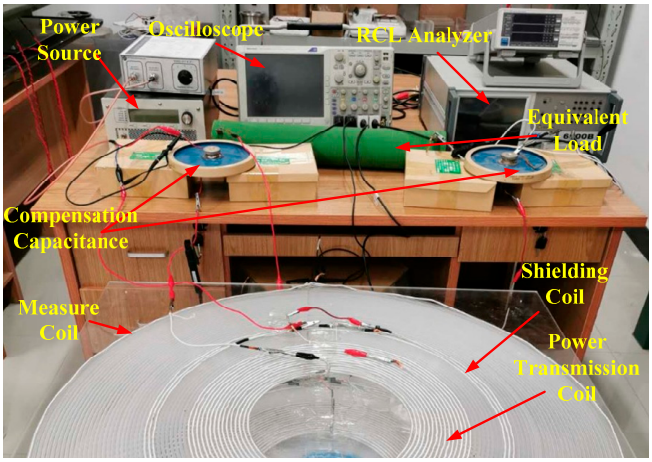

Figure 10. The experiment setup.

So, we can get the mutual inductance between coil X and coil Y.

$$M_{XY} = \frac{L_{T1} - L_{T2}}{4} \tag{53}$$

Once the mutual inductance is obtained, the coupling coefficients can be calculated by Equation (19). The parameters about experiment are listed in Table 1.

Table 1. Parameters in experiment.

Note	Symbol	Value
Primary power-transfer coil inductance	L_1	126.13 ± 2 μH (changing with frequency)
Secondary power-transfer coil inductance	L_3	121.53 ± 2 μH (changing with frequency)
Turns of power-transfer coils	N_p	15
Inner and outer diameter of power transfer coils	D_1, D_2	300 mm, 496 mm
Primary shielding coil inductance	L_2	15.15 ± 0.5 μH (changing with frequency)
Secondary shielding coil inductance	L_4	15.3 ± 0.5 μH (changing with frequency)
Turns of shielding coils	N_s	3
Inner and outer diameter of shielding coils	D_3, D_4	552 mm, 580 mm
Distance between adjacent turns	d	7 mm
Transmission distance	h	150 mm
The equivalent load	R_L	50.1 Ω
Coupling coefficients	k_{12}, k_{13}, k_{14}, k_{23}, k_{24}, k_{34}	0.315, 0.205, 0.163, 0.161, 0.174, 0.312

For the reason that the permeability and conductivity of PMMA are same with air and its permittivity is close to the permittivity of air, we treat air as the only power transmission medium in theoretical calculation.

Before the test, we make use of the LCR analyzer to get the ESR of the coils and connection lines. The ESR is approximately linearly related to frequency, so we can get:

$$R_1 = R_3 = (0.3 + Kf)\,\Omega\,K = 1.52\,\mathrm{MHz}^{-1}, f \in (0.05, 0.4)\,\mathrm{MHz} \tag{54}$$

When the circuit in resonance state, we make use of the oscilloscope to get U, I_1 and I_3. Then we can calculate the power transmission efficiency η as:

$$\eta = \frac{R_L I_3^2}{U I_1} \tag{55}$$

Through changing the compensation capacitance, the relationship between power transmission efficiency and resonance frequency can be obtained.

From Figure 11, it is obvious that shielding coils will reduce the power transfer efficiency when the frequency is low, and the efficiency becomes close with the increase of frequency. When $N_s = 3$, the inductive structure performs better than the series-opposing structure. The reasons for these phenomena are that the equivalent mutual inductances for the systems with shielding coils become less and M_{PS} is less than M_{eq} for the systems we research. The results agree well with the circuit analysis and FEA analysis. Further, we can find that the most of experiment results are smaller than the corresponding theoretical results. The reason can be that we ignored the loss in capacitors and shielding coils. The difference between experimental results and theoretical results in Figure 11b,c is larger than the difference in Figure 11a. We think there are two reasons for this phenomenon. One such reason is that coils in experiment are not totally symmetrical and their inductance varies with the working frequency. Thus it's hard to make the power transmission coils in resonance condition at the same time. Another reason is the instrumental error and measurement error. Because of these factors, the result that the maximum difference is below 6% is acceptable.

Because every turn of coils is coaxial, the electric field is coaxial too. We can get the open circuit voltage of one turn measure coil and its radius r, so the electric field (E_{exp}) can be calculated when the output current is 1 A.

$$E_{\mathrm{exp}} = \frac{U_{ocv} I'}{2\pi r I_3}\, I' = 1\,\mathrm{A} \tag{56}$$

When the resonance frequencies for three kinds of structures are around 200 kHz, the power transmission efficiency for no-shielding structure, series-opposing structure and inductive structure are 93.06%, 87.57%, and 92.87% respectively. Ignoring the influence of frequency when the electric field is compared, the theoretical and experimental results are presented in Figure 12.

From Figures 11 and 12, it can be obtained that the electric field excited by series-opposing structure is about 60% of the no-shielding structure and the electric field excited by inductive structure is about 35% of the no-shielding structure. As for the power transmission efficiency, the efficiency of inductive structure is very close to the no-shielding structure when the frequency is higher than 200 kHz and the efficiency for series-opposing structure decreases with the increase of shielding effect. So, it is reasonable to get the conclusion that the inductive structure WPT system produces the weakest EMF in surrounding space when the efficiency is same. Further, the EMF in the primary side is stronger than the secondary side for the reason that the current in the primary coils is higher than the current in secondary coils. Because coils in the experiment are not totally symmetrical, and the inductance of coils changing with the working frequency, it's hard to make the power transmission coils in resonance condition at the same time. Once the resonance state is disturbed, the reactive power will increase fast and the current becomes large. So, the EMF will be stronger than in ideal condition. Further, some iron clips that will increase the magnetic field are around coils, and there are measurement errors. Because

of these factors, the phenomenon whereby theoretical results are lower than the experimental results is reasonable and acceptable.

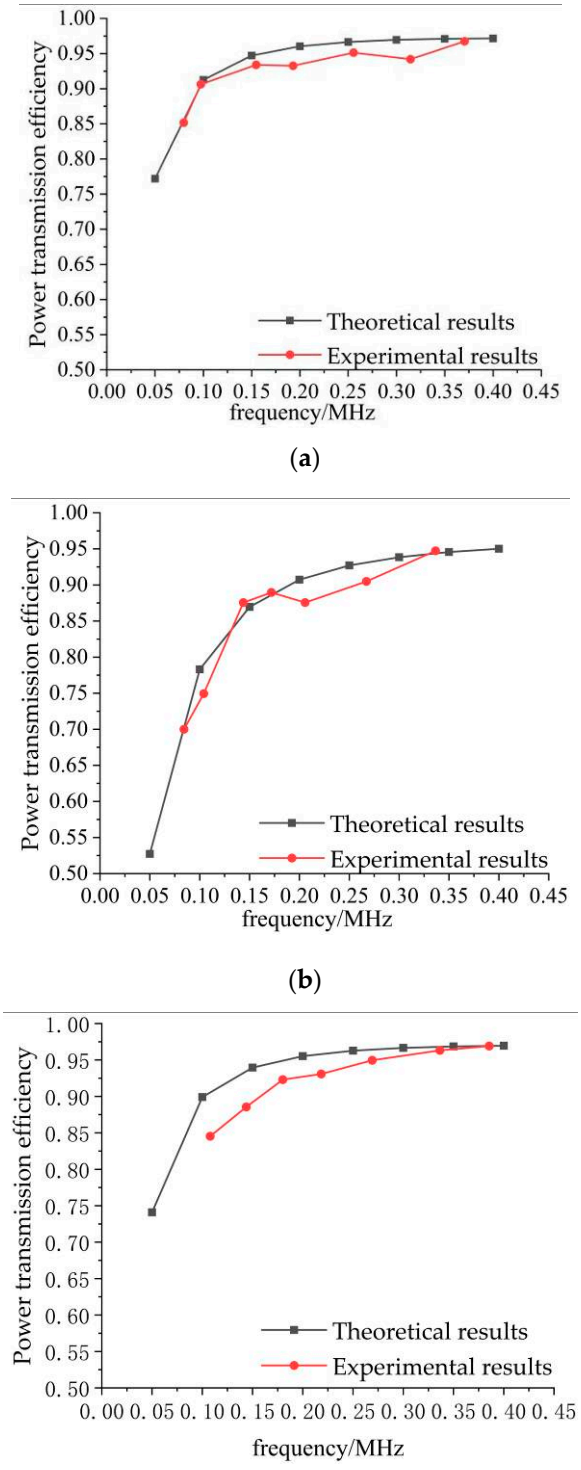

Figure 11. The power transmission efficiency changes with the resonance frequency: (**a**) the WPT system without shielding coils; (**b**) the series-opposing structure WPT system; (**c**) the inductive structure WPT system.

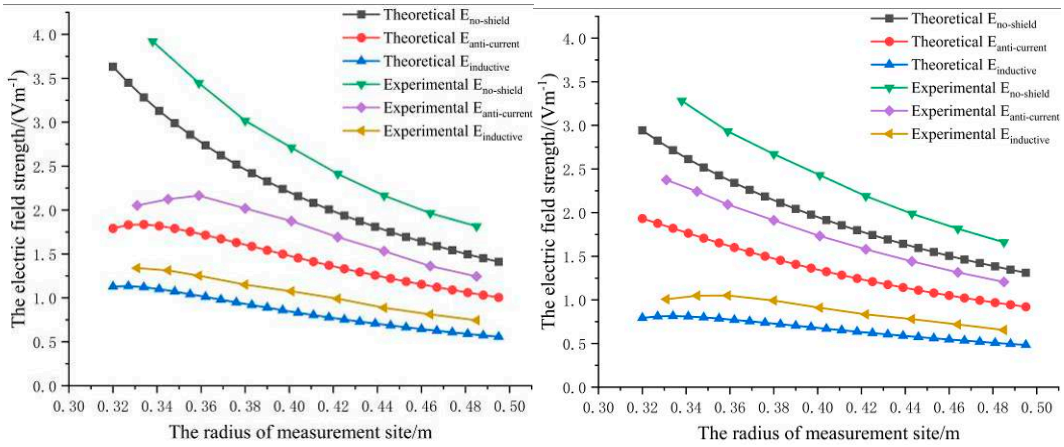

Figure 12. The electric field strength excited by three structure WPT systems: (**a**) The measurement sites are on the plane where the primary coils are located; (**b**) The measurement sites are on the plane where the secondary coils are located.

In total, shielding coils can reduce the EMF excited by WPT system efficiently and the inductive structure performs better than the series-opposing structure for the system we researched. The theoretical analysis is confirmed by experimental results.

5. Conclusions

Shielding coils reduce stray EMF excited by WPT systems efficiently and make the charging process safer. Further, they have the advantages of simplicity, lightness, cheapness, and no additional control strategies. In this paper, the series-opposing structure and inductive structure are compared by the equivalent circuit model and FEA. The results show that the turn of shielding coil plays a key role for the series-opposing structure but can't affect the performance of the inductive structure. When N_s = 3, the electric field excited by series-opposing structure is approximately 60% of the no-shielding structure and the electric field excited by the inductive structure is about 35% of the no-shielding structure. The analysis results were supported by the simulation and experiment.

The strong point of the series-opposing structure is that the shielding effectiveness can be adjusted conveniently, but its mutual inductance decreases fast with the increase of shielding coils' turn. Further, its shielding effectiveness is inferior compared with the inductive structure. The advantage of the inductive structure is that it can attenuate stray EMF efficiently with minor efficiency decreasing. Its shielding effectiveness keeps constant if the position doesn't change. So, it's hard to adjust the effectiveness. If the WPT system meets the power transmission efficiency, we'd better choose the suitable structure considering the human body healthy and electronic devices safe. This paper provides the characteristics and the rule of shielding effectiveness of these two kinds of shielding coils. Accordingly, these findings will hopefully support the choice of shielding method in engineering applications.

Author Contributions: Y.W. conceived the study and wrote the manuscript; B.S. and Z.M. analyzed the theoretical results and reviewed the manuscript. All authors have read and agreed to the published version of the manuscript.

Funding: This research was funded by National Science Foundation of China (Grant No.: 51179159; 61572404) and the Shaanxi Province Youth Science and Technology New Star Project (Grant No. 2016KJXX-57).

Conflicts of Interest: The authors declare no conflict of interest.

References

1. Patil, D.; McDonough, M.K.; Miller, J.M.; Fahimi, B.; Balsara, P.T. Wireless Power Transfer for Vehicular Applications: Overview and Challenges. *IEEE Trans. Transp. Electrif.* **2017**, *4*, 3–37. [CrossRef]

2. Rozario, D.; Azeez, N.A.; Williamson, S.S. Comprehensive review and comparative analysis of compensation networks for Capacitive Power Transfer systems. In Proceedings of the IEEE International Symposium on Industrial Electronics, Santa Clara, CA, USA, 8–10 June 2016; pp. 823–829.
3. Dai, X.; Li, X.; Li, Y.; Hu, A.P. Maximum Efficiency Tracking for Wireless Power Transfer Systems with Dynamic Coupling Coefficient Estimation. *IEEE Trans. Power Electron.* **2018**, *33*, 5005–5015. [CrossRef]
4. Zaheer, A.; Neath, M.; Beh, H.Z.; Covic, G.A. A dynamic EV charging system for slow moving traffic applications. *IEEE Trans. Transp. Electrif.* **2017**, *3*, 354–369. [CrossRef]
5. Xiao, C.; Cheng, D.; Wei, K. An LCC-C Compensated Wireless Charging System for Implantable Cardiac Pacemakers: Theory, Experiment, and Safety Evaluation. *IEEE Trans. Power Electron.* **2018**, *33*, 4894–4905. [CrossRef]
6. Lin, M.; Li, D.; Yang, C. Design of an ICPT system for battery charging applied to underwater docking systems. *Ocean Eng.* **2017**, *145*, 373–381. [CrossRef]
7. Kan, T.; Mai, R.; Mercier, P.P.; Mi, C.C. Design and Analysis of a Three-Phase Wireless Charging System for Lightweight Autonomous Underwater Vehicles. *IEEE Trans. Power Electron.* **2018**, *33*, 6622–6632. [CrossRef]
8. Tan, L.; Li, J.; Chen, C.; Yan, C.; Guo, J.; Huang, X. Analysis and performance improvement of WPT Systems in the environment of single non-ferromagnetic metal plates. *Energies* **2016**, *9*, 576–592. [CrossRef]
9. Wen, F.; Huang, X. Optimal Magnetic Field Shielding Method by Metallic Sheets in Wireless Power Transfer System. *Energies* **2016**, *9*, 733–748. [CrossRef]
10. Lu, M.; Ngo, K.D.T. Attenuation of Stray Magnetic Field in Inductive Power Transfer by Controlling Phases of Windings' Currents. *IEEE Trans. Magn.* **2017**, *53*, 1–8. [CrossRef]
11. Lu, M.; Ngo, K.D.T. Comparison of Passive Shields for Coils in Inductive Power Transfer. In Proceedings of the IEEE Applied Power Electronics Conference and Exposition (APEC), Tampa, FL, USA, 26–30 March 2017; pp. 1419–1424.
12. Kiani, M.; Ghovanloo, M. IEEE The Circuit Theory Behind Coupled-Mode Magnetic Resonance-Based Wireless Power Transmission. *IEEE Trans. Circuits Syst. I Regul. Pap.* **2012**, *59*, 2065–2074. [CrossRef] [PubMed]
13. Wang, S.; Gao, D. Power transfer efficiency analysis of the 4-coil wireless power transfer system based on circuit theory and coupled-mode theory. In Proceedings of the IEEE 11th Conference on Industrial Electronics and Applications (ICIEA), Hefei, China, 5–7 June 2016; pp. 1230–1234.
14. Yan, Z.; Zhang, Y.; Kan, T.; Lu, F.; Zhang, K.; Song, B.; Mi, C.C. Frequency Optimization of a Loosely Coupled Underwater Wireless Power Transfer System Considering Eddy Current Loss. *IEEE Trans. Ind. Electron.* **2018**, *66*, 3468–3476. [CrossRef]
15. Wang, S.; Dorrell, D.G.; Guo, Y.; Hsieh, M.F. Inductive Charging Coupler with Assistive Coils. *IEEE Trans. Magn.* **2016**, *52*, 2–5. [CrossRef]